Direct Measurement of the Angular Dependence of the Single-Photon Ionization of Aligned N_2 and CO_2[†]

Isabell Thomann,[‡] Robynne Lock,[‡] Vandana Sharma,[‡] Etienne Gagnon,[‡] Stephen T. Pratt,[§] Henry C. Kapteyn,[‡] Margaret M. Murnane,[‡] and Wen Li*,[‡]

JILA and Department of Physics, University of Colorado and NIST, Boulder, Colorado 80309, and Chemistry Division, Argonne National Laboratory, Argonne, Illinois 60439

Received: March 18, 2008; Revised Manuscript Received: June 10, 2008

By combining a state-of-the-art high-harmonic ultrafast soft X-ray source with field-free dynamic alignment, we map the angular dependence of molecular photoionization yields for the first time for a nondissociative molecule. The observed modulation in ion yield as a function of molecular alignment is attributed to the molecular frame transition dipole moment of single-photon ionization to the X, A and B states of N_2^+ and CO_2^+. Our data show that the transition dipoles for single-photon ionization of N_2 and CO_2 at 43 eV have larger perpendicular components than parallel ones. A direct comparison with published theoretical partial wave ionization cross-sections confirms these experimental observations, which are the first results to allow such comparison with theory for bound cation states. The results provide the first step toward a novel method for measuring molecular frame transition dipole matrix elements.

Introduction

Knowledge of the molecular frame transition dipole $\langle\psi_{\text{ionic}}|\mu|\psi_{\text{neutral}}\rangle$ between neutral and ionic states of molecules is fundamental to understanding photoionization of molecules. The calculation of transition dipole moments is substantially more difficult for bound−free transitions than for bound−bound transitions, because the former require the accurate treatment of the continuum wave function of the free electron.[1] Experimental molecular frame transition dipole matrix elements for photoionization have been determined previously by measurements of rotationally resolved photoelectron angular distributions[2–6] and by coincidence measurements of "fixed-in-space" photoelectron angular distributions following dissociative ionization.[7] In the latter experiments, measurement of the recoil direction of the ion fragment(s) defines the direction of the molecular axis within the constraints of the axial recoil approximation. Although these approaches have produced beautiful and enlightening results, both methods have their limitations. To date, the former approach has only been applied to hydride molecules and to the photoionization of selected high rotational levels of diatomic molecules, where the rotational spacings of the ion are sufficiently large to resolve. The latter approach has been applied to both valence-[8] and inner-shell[9–11] ionization but is limited to systems in which the ion dissociates rapidly. Thus, complementary approaches for determining molecular frame transition dipole matrix elements are highly desirable.

It has long been proposed[9] that a perfectly aligned molecular sample ($\langle\cos^2\theta\rangle = 1$) would enable the direct measurement of the molecular frame transition dipoles for states undergoing nondissociative ionization, which is the dominant process in photoionization. A novel method of breaking the symmetry is to adsorb the molecule onto a surface. In the case of CO, it is possible to monitor the intensity of a particular shape resonance as a function of X-ray polarization to determine if the molecule is lying flat or perpendicular to a surface.[12] However, a molecule adsorbed on a surface is not a free molecule. In the case of gas phase molecules, adiabatic and nonadiabatic alignment methods have been extensively studied over the past decade.[13–15] Adiabatic alignment requires a very strong static electric field or a long laser pulse (picosecond to nanosecond), that slowly aligns the molecular axes along the laser polarization by exerting a torque on the induced dipole. Adiabatic alignment has recently been used in an X-ray absorption experiment to study CF_3Br.[16] Nonadiabatic alignment employs a short laser pulse to excite a coherent rotational wave packet, which undergoes periodic rephasing (revivals) and transiently aligns the molecules. This approach has the advantage of being field free and is therefore more attractive for studying the interaction between nonperturbed free molecules and photons. Nonadiabatic alignment has been used in a recent experiment, to probe alignment effects using EUV (extreme ultraviolet) radiation.[17] Suzuki and co-workers[18] demonstrated the possibility of generating a rotational wave packet by using a one-photon transition. The issue with this type of experiment lies in the low degree of alignment they can produce in molecules. The theoretical limiting value of $\langle\cos^2\theta\rangle$ is 0.6 for a pure parallel transition. In contrast, the adiabatic and nonadiabatic alignment does not have such limit. For example, a very high degree of alignment ($\langle\cos^2\theta\rangle = 0.92$) has been achieved in iodobenzene by Kumarappan et al.[19] Experimental conditions such as molecular rotational temperature and laser intensity can be optimized to increase the degree of alignment. Of course, the method is restricted to molecules with anisotropic polarizability.

In this work we show that by combining nonadiabatic alignment using strong femtosecond pulses with a reaction "microscope"-molecular imaging apparatus, we can use femtosecond soft X-ray pulses to measure the relative single-photon ionization cross-section as a function of molecular alignment. As a result, we can directly obtain the ratio between the parallel and perpendicular molecular frame transition dipoles. We also

[†] Part of the "Stephen R. Leone Festschrift".

* Corresponding author. E-mail: wli@jila.colorado.edu.
[‡] University of Colorado and NIST.
[§] Argonne National Laboratory.

10.1021/jp8023414 CCC: $40.75
Published on Web 08/12/2008

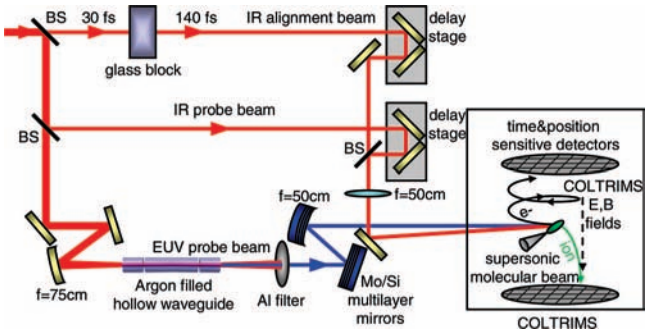

Figure 1. Experimental setup. An IR (800 nm) alignment pulse of duration 140 fs first aligns the supersonically cooled N_2 and CO_2 molecules. Aligned molecules are then ionized by either a delayed, 35 fs, IR pulse or a ~10 fs, 43 eV energy, soft X-ray pulse (blue).

compare the angular dependence of single-photon ionization with soft X-rays to the angular dependence of multiphoton ionization by an intense femtosecond infrared (IR) laser field. We find that the N_2^+ and CO_2^+ multiphoton ionization ion yields are maximized when the molecules are aligned with the polarization axis of an intense IR field. In contrast, for single-photon nondissociative ionization by soft X-rays, the ion yields maximize when the molecules are aligned perpendicular to the polarization of the X-rays. These measurements indicate that the ionizing transitions are predominantly perpendicular for single-photon soft X-ray ionization, and allow a direct comparison with theory for the first time for these systems. Finally, we show that the single-photon dissociative ionization channels $N_2 \rightarrow N^+ + N + e^-$ and $CO_2 \rightarrow O^+ + CO + e^-$ are maximized when the molecules are aligned parallel to the soft X-ray polarization, in contrast to the nondissociative ionization channels. These results provide the first step toward direct measurement of molecular frame transition dipoles from highly aligned molecules in the laboratory frame.

Lepine et al.[17] have performed similar experiments using a combination of short IR pulses to align N_2 and CO_2, and EUV light produced by high-harmonic generation to probe the alignment. The principal difference between their work and our experiment is that their EUV beam was not energy-selected but consisted of all harmonic orders between ~20 and 55 eV. In our experiment, we use multilayer mirrors to select a single harmonic order—the 27th harmonic at ~43 eV—with a few electronvolt bandwidth. This difference is important because the molecular frame transition dipoles, and thus the relative amplitudes of the parallel and perpendicular transitions, are energy dependent. Thus, the larger bandwidth of the previous measurements is expected to smooth out any variations. In addition, although the potential of the approach for threshold (nondissociative) photoionization was discussed, the earlier measurements focused on dissociative ionization processes, and no parent cation yield modulation was observed. Their attempt to observe an alignment dependence of the angle-resolved photoelectron spectrum of N_2 was unsuccessful.

Experimental Section

To measure the single-photon ionization yield during a rotational wave packet revival in a small molecule, subpicosecond soft X-ray pulses are needed because of the short duration of the revival. Therefore, in this experiment we use high harmonic generation by a femtosecond laser to produce ultrafast (≈10 fs) soft X-ray pulses as the source of ionizing radiation. The experimental setup is shown in Figure 1. We use a Ti:sapphire amplifier system producing 2 mJ pulses, at a 2 kHz repetition rate, and with 35 fs pulse duration, and split the output into pump and probe beams. The pump pulse, with intensity $\sim 4 \times 10^{12}$ W/cm^2, is stretched to 140 fs to impulsively align the molecules by creating a rotational wave packet, which periodically exhibits macroscopic field-free alignment around the polarization axis of the pump aligning pulse.[20] The probe beam, with energy 1 mJ, is focused into an argon-filled hollow waveguide to produce a comb of phase matched harmonics.[21] Using two Mo/Si multilayer mirrors and an Aluminum filter (200 nm thick), we preferentially select soft X-ray harmonics centered at ~43 eV (27th harmonic), which are then focused noncollinearly with the pump beam into the molecular sample. The soft X-ray photon flux is estimated to be $\sim 10^8$/s. The relatively large bandwidth of the EUV light precludes the resolution of vibrational (and even electronic) structure in the photoelectron spectra of the N_2^+ and CO_2^+, which have vibrational spacing of ~0.1−0.4 eV. Alternatively, we can use IR light as the probe beam to ionize the molecule using multiphoton strong-field ionization that occurs at laser intensities around 3×10^{13} W/cm^2. Because multiphoton ionization is a more sensitive probe of alignment, we first used the strong field ionization signal to verify our alignment conditions.

To extract the angle dependent ion yield, a molecular supersonic gas jet is placed in a COLTRIMS (Cold Target Recoil Ion Momentum Spectroscopy) reaction microscope,[22] which allows reconstruction of the full momentum vectors of all charged particles resulting from ionization, with coincidence measurement capability. We exploit the COLTRIMS coincidence and momentum imaging capabilities to distinguish different ionization channels. We measure the kinetic energy E_{pe} of photoelectrons detected in coincidence with the respective ions. This allows determination of the ion channel by its vertical ionization energy $E_{ion} = h\nu_{EUV} - E_{pe}$.

The ion yield was probed during the first half-revival for N_2 (4.2 ps) and CO_2 (21.0 ps), where the molecular axis distribution changes from aligned to antialigned. The variation of the angular distribution with delay during a rotational revival is effectively the same as varying the angle between pump and probe polarization at a fixed time delay corresponding to maximum molecular axis alignment. However, by using parallel polarizations in the alignment and ionizing pulses, azimuthal symmetry is maintained at all times, which simplifies the analysis.

Results

Figure 2 shows the photoelectron spectra of N_2 and CO_2, measured in coincidence with N_2^+ and N^+, and CO_2^+ and O^+, respectively, following ionization by 43 eV photons. Within our experimental resolution, these spectra agree with published photoelectron spectra of CO_2 and N_2, showing that single-photon ionization of N_2 results primarily in the population of the X $^2\Sigma_g^+$, A $^2\Pi_u$ and B $^2\Sigma_u^+$ states of N_2^+, and that ionization of CO_2 results primarily in the population of the X $^2\Pi_g$, A $^2\Pi_u$, B $^2\Sigma_u^+$, and C $^2\Sigma_g^+$ states of CO_2^+. The ionization energy of N_2 is 15.6 eV, and the dissociation energy of N_2^+ is 8.7 eV, resulting in a dissociative ionization threshold of 24.3 eV.[23] Thus, with a 43 eV photon, photoelectrons with kinetic energy greater than ~18.7 eV are expected to be correlated with stable N_2^+, whereas photoelectrons with kinetic energy less than ~18.7 eV are expected to be correlated with N^+ fragments. Given our experimental resolution, this assumption is consistent with Figure 2a. Similarly, the ionization potential of CO_2 is 13.8 eV and the dissociation energy of CO_2^+ is ~5.3 eV, resulting in a dissociative ionization threshold of ~19.1 eV. Photoelectrons with kinetic energy greater than ~23.9 eV should therefore be

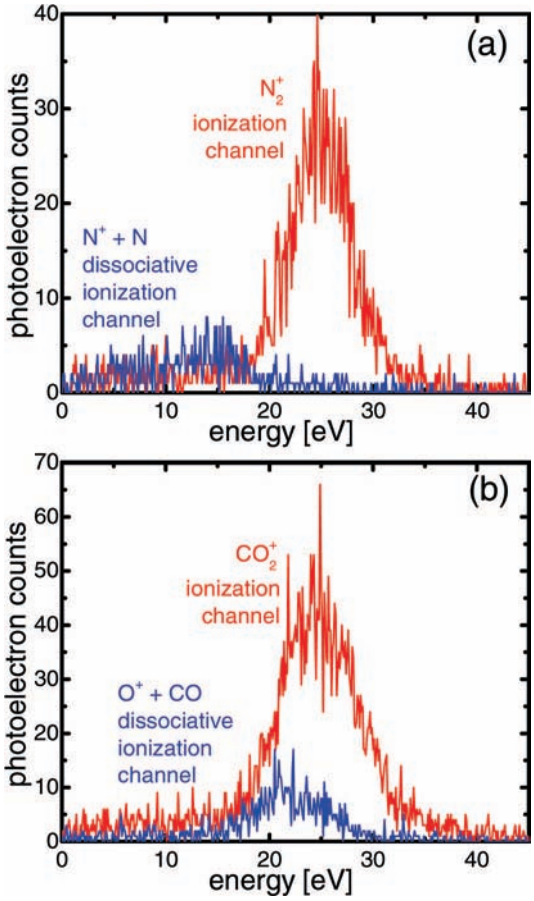

Figure 2. Photoelectron spectra in coincidence with (a) N_2^+ (red) and N^+ (blue) (b) CO_2^+ (red) and O^+ (blue). With coincidence measurement, N_2^+ and CO_2^+ are found at X, A and B state. N^+ is from N_2^+ inner valence states with binding energy >24 eV. O^+ is from CO_2^+ C dissociative state (~19 eV).

correlated with stable CO_2^+. Although this is generally consistent with our observations, in contrast to N_2, some CO_2^+ appears unstable for photoelectron energies up to ~30 eV. This result may simply reflect the bandwidth of the high-harmonic light. In addition, some CO_2^+ appears to be stable for photoelectron energies down to about 18 eV. This observation may simply result from the larger number of internal degrees of freedom in CO_2^+, resulting in a longer lifetime before dissociation, and enabling competing nondissociative decay mechanisms such as fluorescence to stabilize the parent ion. This observation is also consistent with the relatively long dissociation time scale inferred below for the CO_2^+ C state.

The yields for singly ionized N_2 and CO_2 as a function of time delay between the alignment and soft X-ray ionizing pulses, again in the region around the first half revival, are shown in Figures 3 and 4. The insets of these figures also show the ion yields resulting from multiphoton ionization by an intense femtosecond IR field. For the case of multiphoton ionization, it is clear that the N_2^+ and CO_2^+ yields are highest when the molecules are aligned with the polarization of the IR field. However, for the case of single-photon soft X-ray ionization, the ion yield is at minimum when the soft X-ray polarization is parallel to the molecular axis. This surprising contrast clearly demonstrates the difference between multiphoton and single-photon ionization. However, the origin of such difference is not trivial, because the mechanism of multiphoton ionization is still an area of intense investigation[24] and beyond the scope of this paper.

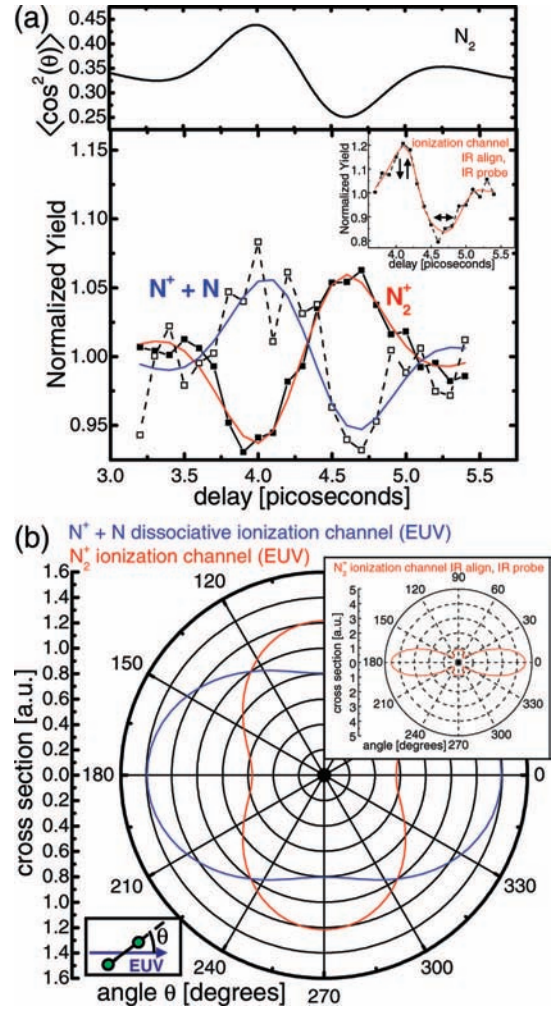

Figure 3. (a) Upper panel: calculated alignment cosine (see text) for N_2 versus time delay. Main panel: EUV ionization yields from transiently aligned N_2. Solid (hollow) symbols: N_2^+ ($N^+ + N$ dissociation). Lines: numerical fitting. Inset: multiphoton (IR) ionization yield of N_2^+ and its numerical fitting. (↕: aligned sample; ↔: antialigned sample). (b) Extracted angular dependence of the EUV ionization yield to N_2^+ and N_2^+ dissociative states (N^+). Inset: extracted angular dependence of multiphoton (IR) ionization of N2. These angular dependences were extracted, as described in the text, from a fit to the delay-dependent yield data shown in (a).

Discussion

Electronic transitions in linear molecules are generally classified as parallel or perpendicular according to whether the dipole is parallel or perpendicular to the molecular axis, with the corresponding selection rule for the electronic angular momentum, Λ, of $\Delta\Lambda = 0$ and $\Delta\Lambda = \pm 1$, respectively. (Note that for the final state in photoionization, Λ includes the electronic angular momentum of the ion and photoelectron.) When the molecule is aligned parallel to the polarization axis of the light, parallel transitions are enhanced, and perpendicular transitions are diminished, whereas the opposite is true if the molecule is aligned perpendicular to the polarization axis of the light. Thus, the time (angular) dependence of the ionization yield is a sensitive probe of the character of the transition dipole, and the angle-dependent yield can be directly related to the molecular frame dipole. Note, however, that limited resolution can complicate the process of extracting the direction of molecular frame dipoles, as several continua can contribute at a given photon energy. For example, if the photoelectron energy resolution is insufficient to resolve different final electronic

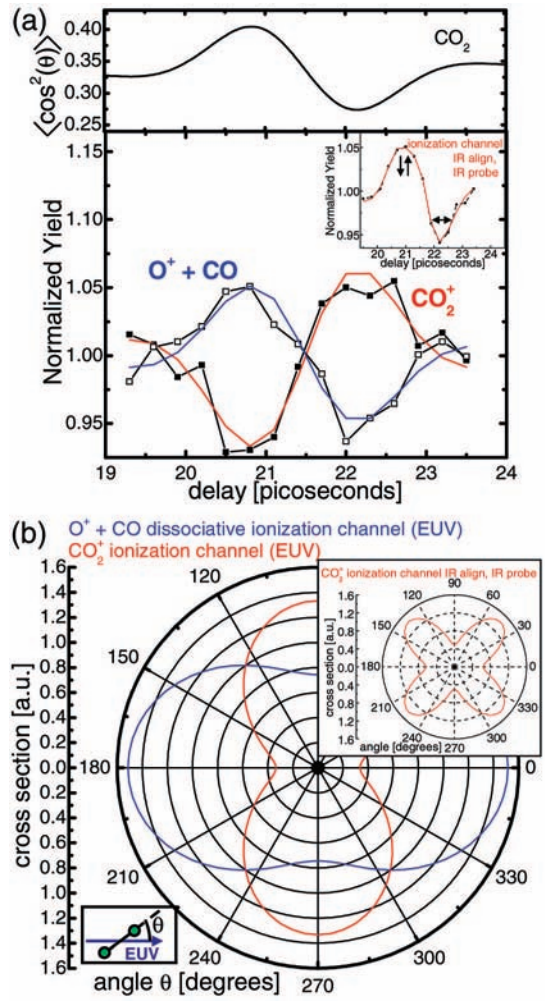

Figure 4. (a) Upper panel: calculated alignment cosine (see text) for CO_2 versus time delay. Main panel: EUV ionization yields from transiently aligned CO_2. Solid (hollow) symbols: CO_2^+ ($O^+ + CO$ dissociation). Lines: numerical fitting. Inset: multiphoton (IR) ionization yield of CO_2^+ and its numerical fitting. (⇅: aligned sample; ↔: antialigned sample). (b) Extracted angular dependence of the EUV ionization yield to CO_2^+ and CO_2^+ dissociative states (O^+). Inset: extracted angular dependence of multiphoton (IR) ionization of CO_2.

states, the N_2 $X^1\Sigma_g^+ \rightarrow N_2^+$ $X^2\Sigma_g^+ + \epsilon p\sigma_u$ or $\epsilon f\sigma_u$ and N_2 $X^1\Sigma_g^+ \rightarrow N_2^+$ $B^2\Sigma_u^+ + \epsilon' s\sigma_g$ or $\epsilon' d\sigma_g$ photoionization processes, which all have the same overall symmetry, will overlap.

To quantitatively determine the angular dependence of soft X-ray photoionization, we first calculate the time dependence of the angular probability distribution $A(\theta,\tau)$ of molecular axes for the rotational revival following the method developed by Ortigoso et al.[20] We use the experimental parameters for alignment pulse duration and laser intensity of 140 fs, 3.5×10^{12} W/cm^2 for CO_2, and 140 fs, 5×10^{12} W/cm^2 for N_2. The degree of alignment of the sample is given by the alignment cosine, i.e., the average of $\cos^2(\theta)$ over the calculated molecular axis distribution: $\langle\cos^2(\theta)\rangle = \int\cos^2(\theta)\, A(\theta,\tau)\, \sin(\theta)\, d\theta / \int A(\theta,\tau) \sin(\theta)\, d\theta$. The calculated alignment cosine for the conditions of the EUV single-photon ionization experiment is given for N_2 and CO_2 in Figures 3a and 4a, upper panel, respectively. Then the ionization yield versus delay τ is given by an angle integral: $\text{Yield}(\tau) = \int A(\theta,\tau)\ \sigma(\theta)\ \sin(\theta)\, d\theta$, where θ is the angle between the direction of polarization of the light and the molecular axes. We expand the angular dependence of the ionization cross-section in terms of Legendre polynomials $\sigma(\theta) = C(1 + \beta P_2(\cos(\theta)) + \gamma P_4(\cos(\theta)) + ...)$. For single-photon ionization, the ionization cross-section only contains the second order term: $\sigma(\theta) = C(1 + \beta P_2(\cos(\theta))$. Note, the β value in the equation is different from the one extracted from photoelectron angular distributions. It simply represents the anisotropy of angular dependence of the ionization cross-section. To remove the effect of possible soft X-ray intensity fluctuations, the yield in the presence of the alignment beam is normalized by the yield without the alignment pulse present. We obtained $\beta = -0.43 \pm 0.13$ by fitting to the N_2^+ ion yield data shown in Figure 3. A theoretical value ($\beta_{\text{theory}} = -0.46$) for this parameter can be derived from the results of recent calculations on the photoionization of N_2 at this energy.[25] To do this, we used the equation: $\beta = (2 - \sigma_{\text{perp}}/\sigma_{\text{para}})/(1 + \sigma_{\text{perp}}/\sigma_{\text{para}})$. σ_{perp} and σ_{para} are the total cross-sections of perpendicular transitions and parallel ones taken from the reference. The theoretical calculations[25] indicate that, at 43 eV, photoionization to the A state makes up more than half of the total ionization cross-section and is strongly perpendicular in character, whereas photoionization to the X and B states has mixed parallel and perpendicular character, resulting in overall perpendicular character for the unresolved continua.

In Figure 3 we also show the N^+ yield from the dissociative channel leading to $N^+ + N$. This process can be separated into transitions leading to two final states—the F $^2\Sigma_g^+$ and $(2\sigma_g)^{-1}$ $^2\Sigma_g^+$ state—with the F $^2\Sigma_g^+$ state dominant. These channels can be separated in our experiment, and thus we can characterize the orientation of their transition dipoles separately: N^+ ions were measured in coincidence with photoelectrons, and energy filters were applied. For the F $^2\Sigma_g^+$ state, the ion energy filter was between 0.08−1.84 eV, and the electron energy filter was between 8−20 eV. For the $(2\sigma_g)^{-1}$ $^2\Sigma_g^+$ state, the ion energy filter was between 1.84 and 5.32 eV, whereas the electron energy filter was between 3.5 and 13.5 eV. We find the β values for the F $^2\Sigma_g^+$ state and $(2\sigma_g)^{-1}$ $^2\Sigma_g^+$ states are 0.47 ± 0.20, and 0.18 ± 0.20, respectively. These correspond to ratios between the perpendicular and parallel dipole contributions of ~1 and 1.54, respectively, using $\sigma_{\text{perp}}/\sigma_{\text{para}} = (2 - \beta)/(1 + \beta)$. These two dissociative channels leading to $N^+ + N$ are the only ones relevant to this study that have been accessible in previous studies using momentum imaging techniques. In experiments with 40.8 eV photons, Hikosaka and Eland[10] have measured a transition ratio $\sigma_{\text{perp}}/\sigma_{\text{para}}$ of 0.23 for the F $^2\Sigma_g^+$ state, and a ratio $\sigma_{\text{perp}}/\sigma_{\text{para}}$ of 0.6 for the $(2\sigma_g)^{-1}$ $^2\Sigma_g^+$ state. Although the ratio for the $(2\sigma_g)^{-1}$ $^2\Sigma^+_g$ state is higher than that for the F $^2\Sigma_g^+$ state in both experiments, the absolute values are quite different. This discrepancy may result in part from the different photon energies in the two experiments.

In Figure 4, we show the O^+ yield from the dissociative channel leading to $O^+ + CO$, as well as the nondissociative CO_2^+ yield. It is obvious that the dissociative process results from a predominantly parallel transition, whereas the nondissociative process results from a predominantly perpendicular one. As in the case of N_2, our results for CO_2 are in agreement with theoretical results ($\beta_{\text{theory}} = -0.43$).[26] Specifically, at 43 eV, perpendicular transitions are expected to dominate photoionization to the X, A, and B states of CO_2^+, whereas parallel transitions are expected to dominate photoionization to the C state of CO_2^+, which mainly predissociates into $O^+ + CO$. We find a β value of -0.67 ± 0.19 for the data shown in Figure 4. These data are for CO_2^+ ions detected in coincidence with electrons in the energy range from 20 to 30 eV, which was done to remove the signal from the IR alone. Because of its low ionization potential of 13.78 eV, CO_2 can be ionized even by the alignment IR pulse. However, because these ions are

TABLE 1: Comparison of Anisotropy Parameters (β) between Experiment and Theory

molecules	ionization channels	β_{expt}	β_{theory}
	N_2^+ (X, A, B)	-0.43 ± 0.13	-0.46
N_2	N_2^+ ($F\ ^2\Sigma_g^+$, $N^+ + N$)	$+0.47 \pm 0.20$	$-/-$
	N^+ $(2\sigma_g)^{-1}\ ^2\Sigma_g^+$, $N^+ + N$)	$+0.18 \pm 0.20$	$-/-$
CO_2	CO_2^+ (X, A, B)	-0.67 ± 0.19	-0.43
	CO_2^+ (C $4\sigma_g$, $O^+ + CO$)	$+0.51 \pm 0.15$	$+0.84$

generated in coincidence with low energy electrons, they therefore can be filtered from the data. We also studied the electron yield for comparison. For electrons with energy between 20 and 30 eV, which are formed in coincidence with both CO_2^+ and $O^+ + CO$, we find a β value of -0.36 ± 0.10. This observation is consistent with the fact that the parallel component for the transition to C state of CO_2^+ is stronger than the perpendicular component. This results in a larger β value than is observed by monitoring CO_2^+ ions, for which the C state does not contribute.

We also obtain the angular dependence of the photoionization cross-section for the dissociative channel $O^+ + CO$. We find a β value of $+0.51 \pm 0.15$ (see Figure 4). The $O^+ + CO$ channel likely proceeds by dissociation from the C $4\sigma_g$ channel of CO_2^+.[17,26,27] Although the O^+ ion signal shows a strong dependence on the alignment of the molecular axis, the O^+ angular distribution at a given delay (or given alignment of the molecular axis to the polarization axis) is essentially isotropic at all delays. This observation is consistent with the results of Lepine et al.[17] In particular, the long lifetime of the intermediate state in this dissociation channel therefore appears to violate axial recoil approximation, leading to an isotropic momentum distribution and making it impossible to determine the transition dipole with conventional methods. However, Dowek et al.[28] reported an anisotropy parameter of ~ 1 for O^+ angular distribution from CO_2 dissociative ionization at 35 eV. Even though this discrepancy between their and our results might be due to the photon energy difference, it needs further investigation to clarify. Theoretically[26,29] it has been predicted that a broad shape resonance structure contributes to the ionization to the C state between 30 and 45 eV. The corresponding continuum orbital is of σ_u symmetry, making this a parallel transition. The experimental β parameter is in agreement with the theoretical value at 43 eV of $\beta_{theory} = 0.84$, which was obtained as described above for N_2. The other partial wave contribution $\sigma_g \rightarrow \pi_u$ is a perpendicular transition and is not affected by the shape resonance. Thus, our method provides a direct way to probe this otherwise elusive shape resonance[30] in free CO_2 molecules.

We summarize extracted experimental anisotropy parameters for different ionization channels and their theoretical values in Table 1.

Conclusion

In conclusion, we have developed a novel method for measuring the direction of molecular transition dipoles. This new method does not require fragmentation of the molecule to determine the direction of the transition dipole and allows measurement of nondissociative bound−free transitions in N_2^+ and CO_2^+ for the first time. Moreover, our approach also allows determination of the direction of the transition dipoles for dissociative ionization, where, for example, the excited lifetime of the state is comparable to or longer than the molecular rotation period, i.e., where the axial recoil approximation breaks down, as we show for the $O^+ + CO$ channel. The method presented here should be also applicable to larger and more complicated molecules and can be extended to measurements of excited molecular states. With increased electron energy resolution, future experiments should also allow selective measurements for individual final states. Finally, as pointed out in the Introduction, a particularly interesting extension of this method will be to measure photoelectron angular distributions of highly aligned molecules. Such measurements will ultimately allow the determination of both quantitative molecular-frame transition dipole matrix elements and their phase-shift differences, i.e., a "complete" ionization experiment.[31]

Acknowledgment. We thank A. Sandhu and C. La-o-vorakiat for their assistance on the experiment. We gratefully acknowledge the financial support from the National Science Foundation and the Department of Energy. S.T.P. was supported by the Chemical Sciences, Geosciences, and Biosciences Division of the Office of Basic Energy Sciences, Office of Science, U.S. Department of Energy under Contract No. DE-AC02-06CH11357.

References and Notes

(1) Lohmuller, T.; Erdmann, M.; Rubner, O.; Engel, V. *Eur. Phys. J. D* **2003**, *25*, 95.
(2) Reid, K. L. *Annu. Rev. Phys. Chem.* **2003**, *54*, 397.
(3) Hockett, P.; King, A. K.; Powis, I.; Reid, K. L. *J. Chem. Phys.* **2007**, *127*, 154307.
(4) Hockett, P.; Reid, K. L. *J. Chem. Phys.* **2007**, *127*, 154308.
(5) Leahy, D. J.; Reid, K. L.; Zare, R. N. *J. Chem. Phys.* **1991**, *95*, 1757.
(6) Park, H.; Zare, R. N. *J. Chem. Phys.* **1993**, *99*, 6537.
(7) Yagishita, A.; Maezawa, H.; Ukai, M.; Shigemasa, E. *Phys. Rev. Lett.* **1989**, *62*, 36.
(8) Rijs, A. M.; Janssen, M. H. M.; Chrysostom, E. T. H.; Hayden, C. C. *Phys. Rev. Lett.* **2004**, *92*, 123002.
(9) Dill, D. *J. Chem. Phys.* **1976**, *65*, 1130.
(10) Hikosaka, Y.; Eland, J. H. D. *J. Phys. B-At. Mol. Opt. Phys.* **2000**, *33*, 3137.
(11) Yagishita, A.; Hosaka, K.; Adachi, J. I. *J. Electron Spectrosc. Relat. Phenom.* **2005**, *142*, 295.
(12) Stohr, J.; Baberschke, K.; Jaeger, R.; Treichler, R.; Brennan, S. *Phys. Rev. Lett.* **1981**, *47*, 381.
(13) Rosca-Pruna, F.; Vrakking, M. J. J. *J. Chem. Phys.* **2002**, *116*, 6567.
(14) Friedrich, B.; Herschbach, D. *Phys. Rev. Lett.* **1995**, *74*, 4623.
(15) Stapelfeldt, H.; Seideman, T. *Rev. Mod. Phys.* **2003**, *75*, 543.
(16) Peterson, E. R.; Buth, C.; Arms, D. A.; Dunford, R. W.; Kanter, E. P.; Krassig, B.; Landal, E. C.; Pratt, S. T.; Southworth, S. H.; L., Y. *Appl. Phys. Lett.* **2008**, *92*, 094106.
(17) Lepine, F.; Kling, M. F.; Ni, Y. F.; Khan, J.; Ghafur, O.; Martchenko, T.; Gustafsson, E.; Johnsson, P.; Varju, K.; Remetter, T.; L'Huillier, A.; Vrakking, M. J. J. *J. Mod. Opt.* **2007**, *54*, 953.
(18) Tsubouchi, M.; Suzuki, T. *J. Chem. Phys.* **2004**, *121*, 8846.
(19) Kumarappan, V.; Bisgaard, C. Z.; Viftrup, S. S.; Holmegaard, L.; Stapelfeldt, H. *J. Chem. Phys.* **2006**, 125.
(20) Ortigoso, J.; Rodriguez, M.; Gupta, M.; Friedrich, B. *J. Chem. Phys.* **1999**, *110*, 3870.
(21) Rundquist, A.; Durfee, C. G.; Chang, Z. H.; Herne, C.; Backus, S.; Murnane, M. M.; Kapteyn, H. C. *Science* **1998**, *280*, 1412.
(22) Gagnon, E.; Ranitovic, P.; Tong, X. M.; Cocke, C. L.; Murnane, M. M.; Kapteyn, H. C.; Sandhu, A. S. *Science* **2007**, *317*, 1374.
(23) Huber, K. P.; Herzberg, G. *Constants of Diatomic Molecules*; Van Nostrand Reinhold: New York, 1979.
(24) Pavicic, D.; Lee, K. F.; Rayner, D. M.; Corkum, P. B.; Villeneuve, D. M. *Phys. Rev. Lett.* **2007**, 98.
(25) Cacelli, I.; Moccia, R.; Rizzo, A. *Phys. Rev. A* **1998**, *57*, 1895.
(26) Cacelli, I.; Moccia, R.; Montuoro, R. *Phys. Rev. A* **2001**, 6301.
(27) Liu, J. B.; Chen, W. W.; Hochlaf, M.; Qian, X. M.; Chang, C.; Ng, C. Y. *J. Chem. Phys.* **2003**, *118*, 149.
(28) Dowek, D.; Lebech, M.; Houver, J. C.; Lucchese, R. R. *J. Electron Spectrosc. Relat. Phenom.* **2004**, *141*, 211.
(29) Lucchese, R. R.; McKoy, V. *Phys. Rev. A* **1982**, *26*, 1406.
(30) Brion, C. E.; Tan, K. H. *Chem. Phys.* **1978**, *34*, 141.
(31) Kessler, J. *Comments At. Mol. Phys.* **1981**, *10*, 47.

JP8023414